Hindawi
Science and Technology of Nuclear Installations
Volume 2018, Article ID 7162387, 14 pages
https://doi.org/10.1155/2018/7162387

Research Article

Modelling of Severe Accident and In-Vessel Melt Retention Possibilities in BWR Type Reactor

Mindaugas Valinčius, Tadas Kaliatka, Algirdas Kaliatka, and Eugenijus Ušpuras

Laboratory Of Nuclear Installation Safety, Lithuanian Energy Institute, Breslaujos St. 3, LT-44403 Kaunas, Lithuania

Correspondence should be addressed to Mindaugas Valinčius; mindaugas.valincius@lei.lt

Received 23 March 2018; Revised 15 June 2018; Accepted 15 July 2018; Published 1 August 2018

Academic Editor: Sevostian Bechta

One of the severe accident management strategies for nuclear reactors is the melted corium retention inside the reactor pressure vessel. The work presented in this article investigates the application of in-vessel retention (IVR) severe accident management strategy in a BWR reactor. The investigations were performed assuming a scenario with the large break LOCA without injection of cooling water. A computer code RELAP/SCDAPSIM MOD 3.4 was used for the numerical simulation of the accident. Using a model of the entire reactor, a full accident sequence from the large break to core uncover and heat-up as well as corium relocation to the lower head is presented. The ex-vessel cooling was modelled in order to evaluate the applicability of RELAP/SCDAPSIM code for predicting the heat fluxes and reactor pressure vessel wall temperatures. The results of different ex-vessel heat transfer modes were compared and it was concluded that the implemented heat transfer correlations of COUPLE module in RELAP/SCDAPSIM should be applied for IVR analysis. To investigate the influence of debris separation into oxidic and metallic layers in the molten pool on the heat transfer through the wall of the lower head the analytical study was conducted. The results of this study showed that the focusing effect is significant and under some extreme conditions local heat flux from reactor vessel could exceed the critical heat flux. It was recommended that the existing RELAP/SCDAPSIM models of the processes in the debris should be updated in order to consider more complex phenomena and at least oxide and metal phase separation, allowing evaluating local distribution of the heat fluxes.

1. Introduction

Nuclear energy is currently counting more than half of a century of its existence. That being said, the technology still keeps advancing and evolving, eliminating more and more safety issues in the nuclear power plants (NPP). However, even extremely rare, severe accidents in NPP must be very carefully investigated, so that consequences would be mitigated in case of such an unlikely event. After the accident in the Fukushima NPP, the whole viewpoint of the nuclear energy organizations including International Atomic Energy Agency has changed and current safety standards require that severe accidents must be covered in the design extension conditions and that must be within the design envelope.

In case of a severe accident, one of the severe accident management strategies for nuclear reactors is the melted corium retention inside the reactor pressure vessel (RPV). The In-Vessel Retention (IVR) of molten corium by external cooling of the vessel lower head was introduced about 25 years ago [1]. It was first applied to two designs of reactors: AP600 [2] and VVER-440 [3]. The VVER-440 case has led to a practical application at the Loviisa plant where IVR is a part of the severe accident management. The AP600 design was not further developed as it was later replaced with the AP1000 design [4], keeping the option of IVR. In parallel, other designs involving IVR were examined, such as APR-1400 [5, 6], SWR-1000 (BWR type, also known as KERENA) [7], and VVER-640 [8]. The concept is also considered for the recent Chinese design CPR-1000.

The IVR strategy is very attractive for several reasons. It ensures that corium is maintained in the vessel, avoiding the presence of large masses of radioactive materials in the containment and the risks of failure of the containment. In principle, external cooling of the vessel appears to be able to extract enough power and is suitable for long-term stabilization of corium. Also the practical design, under its

Table 1: General data of BWR-5 [14–16].

Parameter	Value
Control	109 control rods of SS with Boron carbide or Boron carbide plus Hafnium. Total mass 580 kg.
Fuel	444 fuel assemblies. Matrix 8x8 with 2 water rods. Active core length 3.58 m. Number of fuel rods per assembly 62
Pressure	6.93 MPa nominal
Power (thermal)	2029 MW_t
Steam flow	1100 kg/s
Recirculation pumps	2
Recirculation nominal flow	2565 kg/s
Feed water flow	1097 kg/s
Number of jet pumps	20
Vessel	Made of carbon steel, internally clad with stainless steel; Total height; 20.8 m, diameter 5.30 m; thickness from 0.13 to 0.19 m;

Lower head	radius (cylindrical part) = 2.71 m;
	thickness (cylindrical part) = 0.19 m;
	radius (hemispherical part) =2.87 m;
	thickness (hemispherical part) = 0.19 m;
	heat surface (hemispherical part) = 38.5 m^2;

Mass of Zircaloy	Total mass in the core 27045 kg. Claddings 20745 kg Control rods and fuel boxes 6300 kg

simplest form, appears less expensive than an external core-catcher.

Although this IVR strategy is not new, its potential is still not fully investigated. In order to consolidate the results of these investigations, perform additional studies for the missing parts, and explore the possibilities of IVR in more detail, the HORIZON 2020 project In-Vessel Melt Retention Severe Accident Management Strategy for Existing and Future NPPs (IVMR) [9] was initiated.

The main objective of this article is to investigate various modes of ex-vessel heat transfer and to make a comparison between them. A numerical study of severe accident in the nuclear reactor and the analysis of corium retention inside the reactor pressure vessel are presented. A full plant model of a ~2000 MW thermal power BWR reactor was used and large break Loss of Coolant Accident (LOCA) with total failure of cooling water injection was assumed. Full accident sequence from normal operation conditions to core heat-up, melting, and relocation into lower head was modelled. The ex-vessel cooling was investigated with the available options of the heat transfer modes in the RELAP/SCDAPSIM computer code.

2. Selection of Accident Scenario for the Analysis

The analysis of IVR strategy for BWR type NPP is performed in the frame of IVMR project. As a basis for the analysis the generic BWR model of General Electric BWR-5 reactor installed in Mark-II containment, developed in the frame of the international SCDAP Development and Training Program (SDTP) [11–13], was used. The most important features of this modelled generic BWR-5 reactor are presented in the Table 1.

The general practice suggests that in the safety analysis the worst case scenario should be investigated. For a BWR type reactor, a scenario with the large break LOCA is considered to lead to the worst consequences in the shortest time. In this study, a guillotine break of external circulation pump suction pipe, LOCA without injection of cooling water due to the failure of the Emergency of Core Cooling Systems (ECCS), is considered. The main assumptions for this scenario are as follows: at time moment t = 0 s reactor is shut down (SCRAM'ed), main coolant pumps are tripped, and main steam Isolation valves are closed; cooling water are not supplied during all accident scenario. This is a hypothetical scenario in order to cause the fast core melt and observe the slumping of melted materials to the lower head, which leads to heating of the bottom of the RPV. The containment is modelled and external cooling of the reactor vessel is considered. The technical measures for supplying the water into the reactor cavity are not analyzed in this study. It was assumed that the cavity is filled before the meltdown and slumping of the melted materials into the reactor lower head.

3. RELAP/SCDAPSIM Model Description

The RELAP/SCDAPSIM computer code is widely used in the world to simulate the severe accidents [17, 18]. Computer code consists of three separate modules: RELAP5 calculates thermal hydraulics, SCDAP calculates core heat-up,

oxidation, and degradation, and COUPLE is used to calculate the heat-up of reactor core material that slumps into the lower head of the RPV. The COUPLE module solves two-dimensional, finite-element based heat transfer problem. This module takes into account the decay heat and initial internal energy of slumped debris and then calculates the transport by conduction of this heat in the radial and axial directions to the wall structures and water surrounding the debris. The COUPLE module solves the following two-dimensional energy equation:

$$(1-\varepsilon)\,\rho_D c_D \frac{\partial}{\partial t}(T) = \frac{\partial}{\partial x}\left(k_e \frac{\partial T}{\partial x}\right) + \frac{\partial}{\partial y}\left(k_e \frac{\partial T}{\partial y}\right) + Q \quad (1)$$

where ρ_D is density of debris particles (kg/m^3); c_D is heat capacity of debris particles (J/kg·K); k_e is effective thermal conductivity (W/m·K); Q is volumetric heat generation rate (W/m^3); T is temperature of mixture of debris and interstitial fluid (K); ε is porosity (pore volume/total volume).

The RELAP/SCDAPSIM input deck, which was used for large LOCA simulation in this work, initially was developed by the regulatory body in Mexico (CNSNS) [11, 12] for Laguna Verde NPP in Mexico. The detailed nodalization scheme and explanation of the model is presented in [13]. This input deck was modified, and the ex-vessel model was appended in order to simulate heat transfer through the vessel wall by flooding the reactor cavity and submerging the RPV in water. The supply of feed water, turbine, suppression pool, and control rod drive system are represented by boundary conditions. Four fuel rods channels represent the reactor core and each fuel rod is nodalized with 13 axial nodes to model heat transfer and mass distribution in the core. Boundary conditions that represent the primary containment at constant pressure are fixed to simulate the break-in the recirculation loop with the time-dependent volumes that are connected to the valves. These valves are used to simulate breaks in the recirculation lines (from RPV side and circulation pump side). These valves are open at the beginning of the calculation.

In this work, the heat transfer to the ex-vessel was investigated as a standalone simulation, separated from the full plant simulation. The reason for this separation was to eliminate all the uncertainties arising from the feedback between corium relocation and different mode of vessel cooling, time step, etc. Since the main objective of this work was to investigate various modes of ex-vessel heat transfer and to make a comparison between them. Therefore, the results of a full plant accident scenario simulation were used as an input data for simplified ex-vessel cooling model. The main parameters were the masses, composition, and the decay heat of the corium in the lower head.

Similar model and investigations are presented in [19]. However, in this article, it was reported that for the long-term simulation the problems of the heat transfer in the lower head occurred and calculations of the RELAP/SCDAPSIM code crashed. For our calculations the model was improved. In [19] presented problems were avoided by adjusting the time step ratio between the thermal-hydraulic calculations and 2D finite-element solver for the heat transfer in the lower head and setting it to be equal to 1.

In the RPV ex-vessel model the in-vessel hydrodynamic volume receives the corium slumps, and finite-element mesh is used to calculate the heat transfer from the corium to walls and structures. The convective boundary is then connected to the external surface of the RPV lower head, and the heat from COUPLE finite-element mesh is transferred to hydrodynamic volumes of RELAP5 code, representing the ex-vessel. There are two different modes of ex-vessel in RELAP/SCDAPSIM:

(a) The first one is RELAP5 based convective heat transfer from the external vessel wall to the hydrodynamic volume. The heat transfer coefficient depends on the flow regime in the hydrodynamic volume, void fraction, and all other parameters. The scheme of this model using this method is shown in Figure 1(a).

(b) The second is a special ex-vessel model implemented in COUPLE code, which then uses heat transfer as a function of contact angle of a curved downward facing structure, such as RPV lower head. This model using this approach is presented in Figure 1(b).

In the case of the ex-vessel model with RELAP5 heat transfer mode (see Figure 1(a)), the model consists of 2 time-dependent volumes, 2 single volumes, one vertical pipe component, and a time-dependent junction. Time-dependent volumes used in order to give the boundary conditions for the developed model. 2 single volumes are used as the buffering volumes in the model. Vertical pipe component represents the available volume around ex-vessel. Pipe components have 10 internal nodes (see Figure 1(a)). Each node is connected to a separate segment of the COUPLE mesh. In order to have more precise calculation results each node has flow area and height is different, following the shape of the COUPLE the mesh. The height of the first nodes is increasing going from the bottom to the top of the lower head.

In the case of the ex-vessel model with COUPLE heat transfer mode (Figure 1(b)), a heat transfer is described as a function of contact angle. In this case only one hydrodynamic volume can be connected as a heat sink (limitation of the RELAP/SCDAPSIM MOD 3.4 code). COUPLE code then calculates the contact angle by the shape of the mesh and applies the heat flux, according to the temperature difference between the sink and the COUPLE wall. The sink temperature is chosen to be either saturation temperature by the pressure in that volume or 10 K below the saturation temperature. A separate variable is needed for COUPLE to track the water level in the ex-vessel volume. This variable can be set by the user as a constant (e.g., always full), or it can be a function of time or void fraction in ex-vessel volume or any other option chosen by the user. If the node is calculated to be uncovered (e.g., level variable is 1 m, and the node is at the elevation of 1.5 m), the user-defined heat transfer coefficient for dried-out surface is applied.

The correlation for heat transfer in COUPLE ex-vessel model was obtained from US Nuclear regulatory commission (NRC) subscale boundary layer boiling (SBLB) tests (NUREG/CR6507) [20]. The heat flux depending on contact angle and temperature difference (for model illustrated in

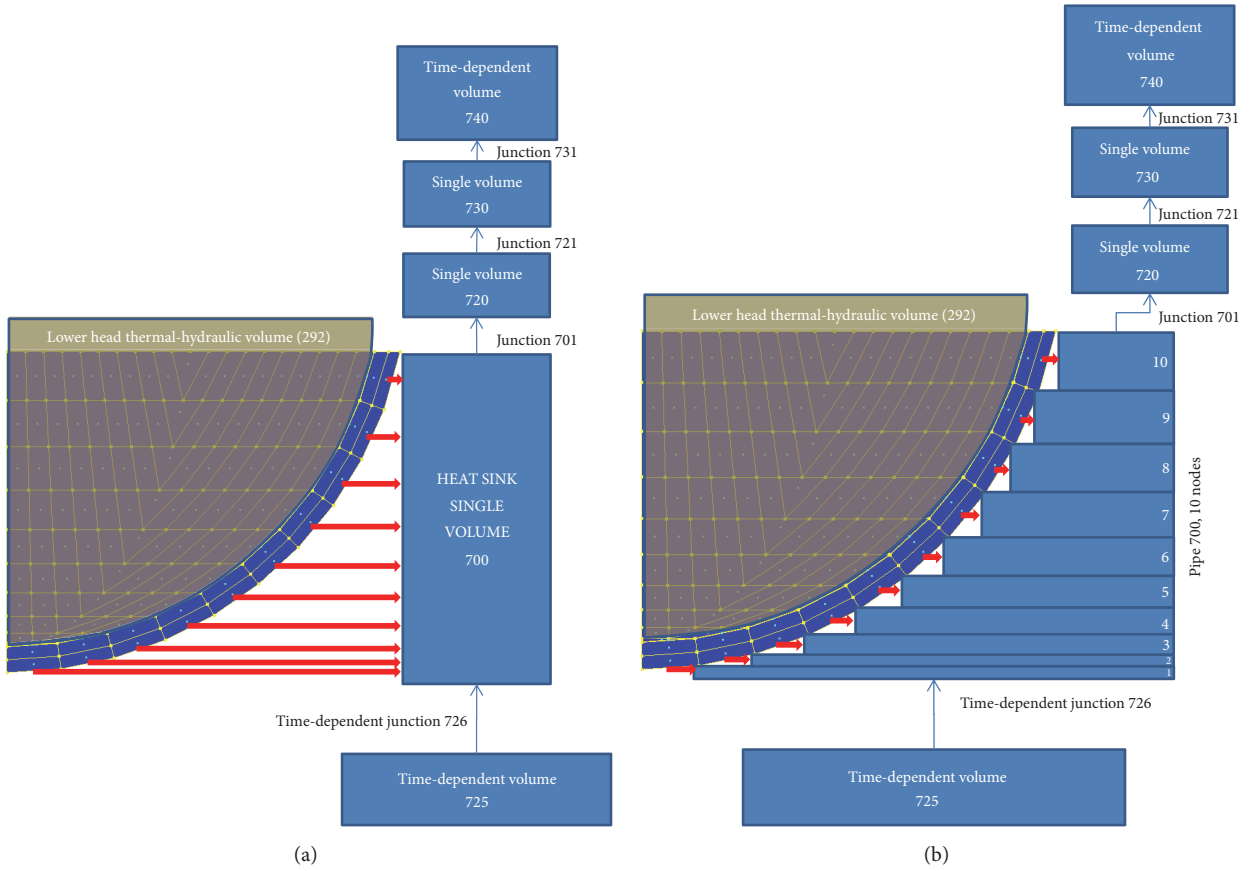

FIGURE 1: Scheme of the COUPLE lower head model with (a) RELAP5 heat transfer; (b) COUPLE heat transfer.

Figure 1(b)) is presented in Figure 2. The peak of each curve means that the CHF has been reached, and the CHF value can be read from y-axis.

The analytical equation of critical heat flux as a function of contact angle (θ) and degree of subcooling (ΔT_{sub}) is defined by (2) [10]. This equation is implemented into the COUPLE code, and the user can choose to apply either saturated or $\Delta T_{sub} = 10$ K subcooled conditions. The resulting critical heat flux of both available options under atmospheric conditions is presented in Figure 3. It is obvious from this figure that using the saturated boiling curve is more conservative assumption for the critical heat flux.

$$q_{chf} = 0.4\left(1 + 0.021\theta - (0.007\theta)^2\right)\left(1 + 0.036\Delta T_{sub}\right) \quad (2)$$

where q_{chf} is critical heat flux (W/m^2); θ is contact angle (deg.); ΔT_{sub} is degree of subcooling (K).

4. Results and Discussion

The objective of the analysis was to investigate the effectiveness of ex-vessel cooling, so that the RPV would stay intact. The main parameter for such evaluation was the wall temperature of the RPV wall. It was assumed that if temperature of the wall reaches the melting temperature of carbon steel (1723 K) the geometry is assumed as melted. The residual wall thickness of the RPV was derived from these results. It was calculated by assuming linear temperature gradient in the vessel wall and from the initial wall thickness (0,19 m) subtracting the thickness of the wall having higher temperature than melting point.

The accident sequence begins from the steady-state conditions, which are tuned to be as close as possible to the reactor design values. The main operational parameters in steady-state operation before the accident were assumed according to the initial conditions presented in Table 1.

The LOCA occurs at the time = 0 s, and at the same moment the feed-water stops. The failure of emergency water supply was assumed. Reactor emergency shutdown (SCRAM) occurs immediately. The key events of the accident sequence are presented in Table 2.

4.1. Processes in the Core. During the steady state, the heat from the core is transferred to the coolant via boiling. After guillotine break of cold leg (large LOCA), the water is rapidly discharged through the broken pipe and the water level in the RPV decreases. The discharge flow rate through the break and collapsed water level in the reactor core are shown in Figures 4 and 5, respectively. Due to the water loss, the reactor gets depressurized and the behavior of steam dome pressure is presented in Figure 6.

After large LOCA is initiated, the top of active fuel is uncovered in 32 seconds after the break and fully uncovers

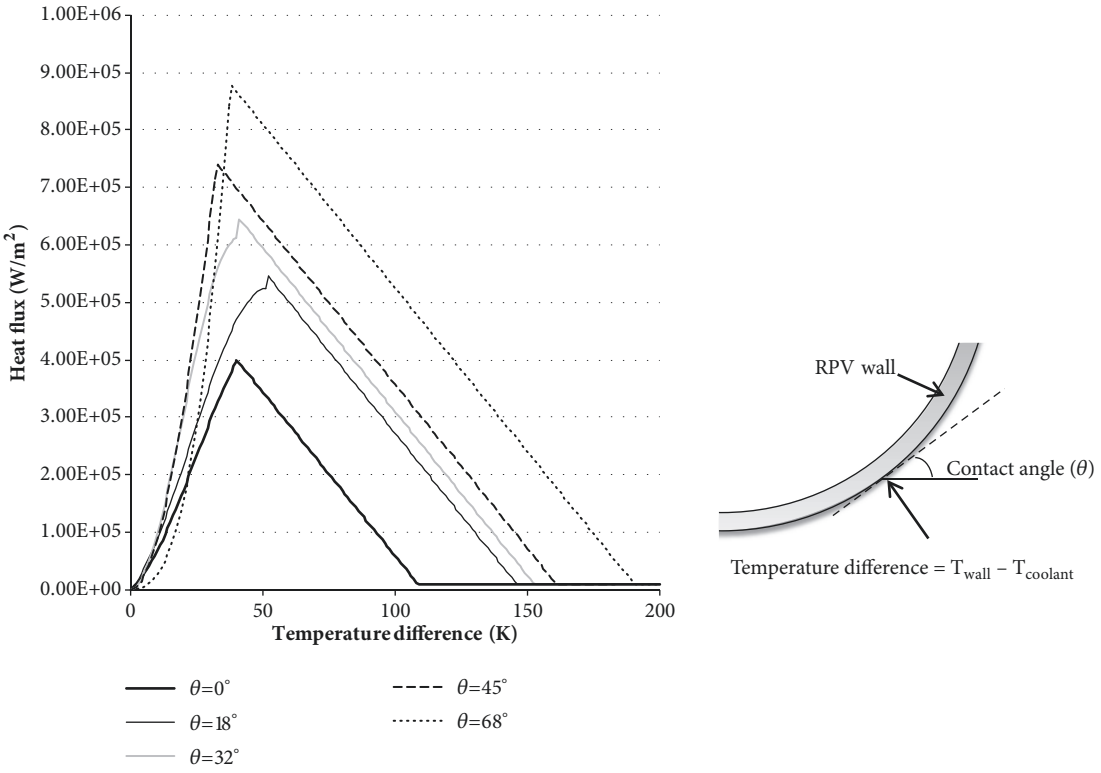

Figure 2: Heat flux as a function of temperature difference and contact angle for COUPLE heat transfer under saturated boiling conditions [10].

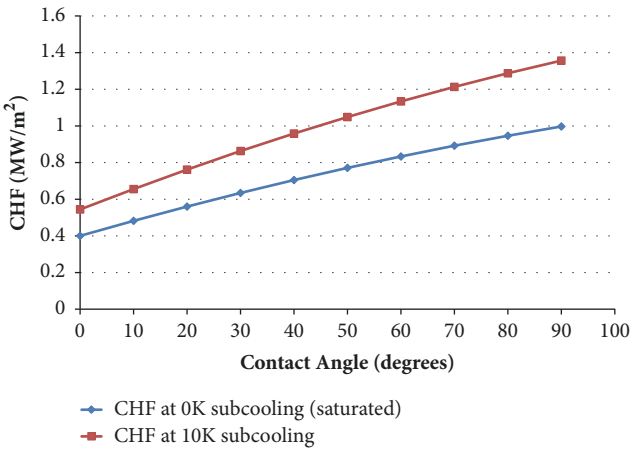

Figure 3: Critical heat flux at atmospheric pressure for both subcooling options in COUPLE heat transfer correlation.

Table 2: Key events of accident sequence.

KEY EVENT	TIME (s)
LOCA	0
Reactor emergency shutdown (SCRAM) initiating (evaluating system delay)	0.2
Turbine trip initiating	0.2
Trip of recirculation pumps initiating	0.3
Core Uncovers/ First heat up of the core	32
Core fully uncovered	50
Oxidation onset	292
$T_{cladding}$ = 1473 K (1200°C)	421
Start of core relocation to lower head	847
Dry out of the lower head	3000

in 50 seconds. After the fuel is uncovered, the heat-up of the fuel rods takes place. The peak cladding temperature is shown in Figure 7. The first rupture due to ballooning occurs in 421 s after the accident. In case of no ECCS in operation as it was assumed in our work, the heat-up of the reactor core progresses and ends up with melting of the core materials and relocation of the debris into the lower head.

The relocation of the corium to the lower head starts at t = 847 s after beginning of the accident. The drop of significant amount of UO_2 debris into lower head leads to more rapid decrease of the water level (at 2600 s after the beginning of the accident). The remaining water in the lower head (as presented in Figure 5) fully evaporates in 3000 s after the beginning of accident, as it is heated by slumped debris.

4.2. Relocation and Decay Heat of Corium in Lower Head. Melting and relocation of the core begin with the lighter metals, and the earliest slumps of debris contain mainly Fe and B_4C absorber and small quantities of Zr and ZrO_2. The first slump is observed at 847 s after the beginning

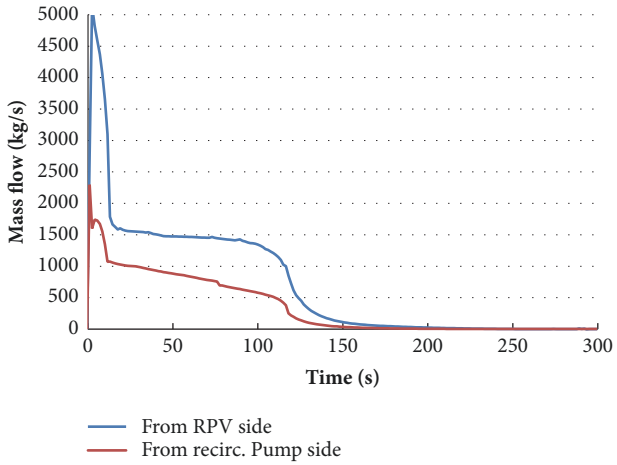

Figure 4: Water discharge flow rate through the break (both ends of the pipe).

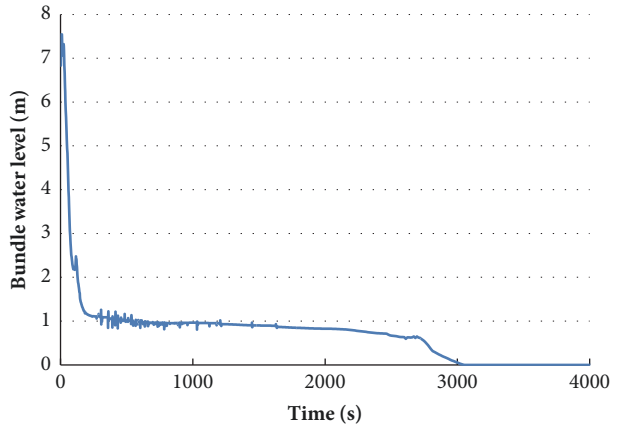

Figure 5: Water level in the RPV.

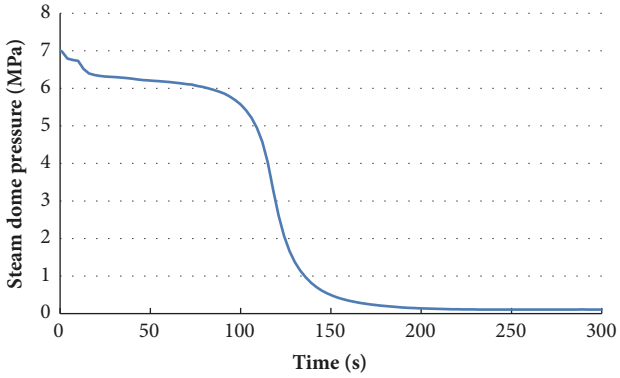

Figure 6: Steam dome pressure.

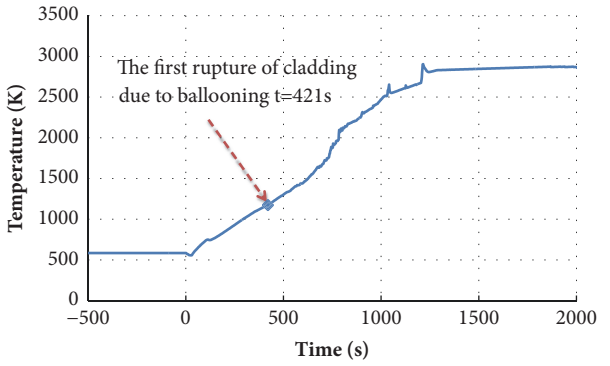

Figure 7: Peak cladding temperature of the core.

of the accident. The slumping of debris to the lower head by material type is shown in Figure 8. Due to limitations of RELAP/SCDAPSIM MOD 3.4 code, the materials in the lower head takes the positions and stay in the order it was relocated. As slumped materials start melting in the lower head, RELAP/SCDAPSIM treats them as a single homogenous liquid pool (see Figure 9), with uniform properties. In reality, complex transient processes take place in debris bed and, after stratification, 2- or 3-layer configuration is formed, depending on the debris composition [21] (as shown in Figure 9). In our calculations, since the light metal is the first to slump into the lower head of RPV, these metals (Fe, B_4C) always stay at the bottom. Above this layer, the debris containing Zr, ZrO_2, and UO_2 builds up later. The origin of all the materials is only the reactor core elements, specifically fuel assemblies, control rods, and channel boxes, because RELAP/SCDAPSIM does not have any additional models to include other internal RPV structures (i.e., core plate, control rod guide tubes, and instrumentation tubes in the lower head) into the debris bed. The only structure considered in the model is the RPV wall, but wall ablation is not considered. The aspect of debris stratification is covered in Section 4.4, where the heat transfer from metal/oxide layers is investigated analytically.

The main task of this analysis is to cope with the decay heat in debris and to achieve proper cooling of the lower head. The decay heat in the reactor core and the corium in the lower head are presented in Figure 10. Each sudden "step" in the chart means that a portion of UO_2 fuel has slumped from the reactor core into the lower head.

4.3. Ex-Vessel Cooling. In our case the reactor cavity outside RPV is assumed to be filled with water before the debris starts slumping into the lower head. The water supply stops after filling the reactor cavity just a bit above the lower head. The total of ~170 m^3 of water is needed to reach this level from the bottom of the reactor pit. The accident management actions as water supply after the accident was not in the scope of this analysis.

Although there is no actual mixing of the materials modelled by RELAP/SCDAPSIM, the heat transfer in the debris bed is simulated not only by conduction, but also by convection. RELAP/SCDAPSIM achieves this by calculating the quantity of liquefied debris and treats it like one well-mixed molten pool with uniform power density and melting temperature. This molten pool has the "effective heat transfer

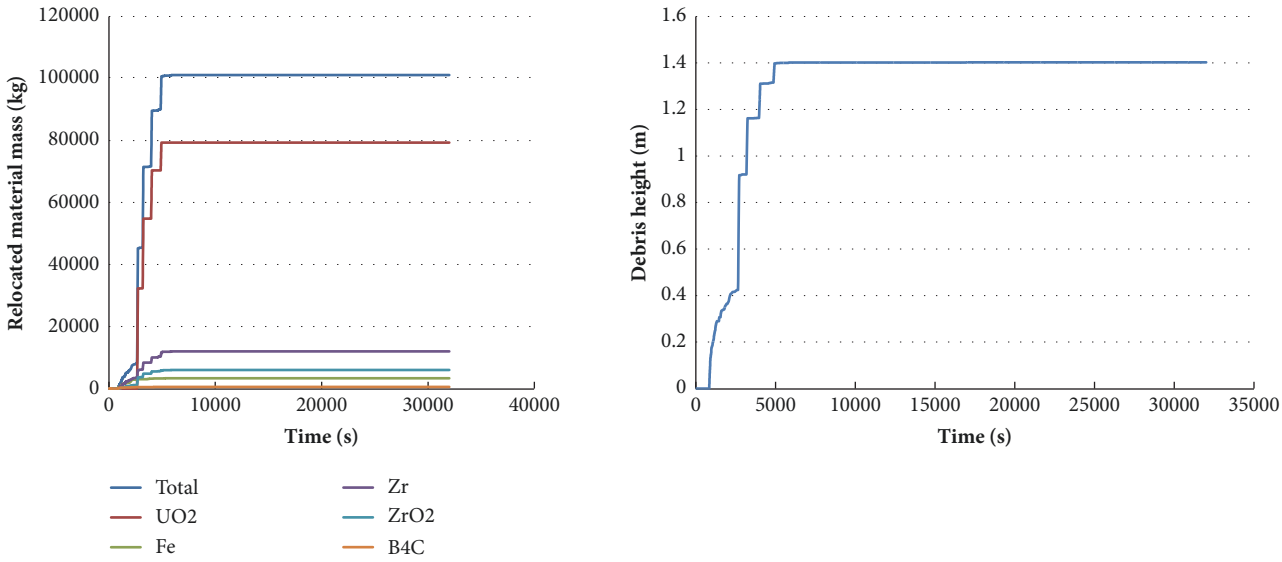

Figure 8: Mass of different materials and debris height in the lower head.

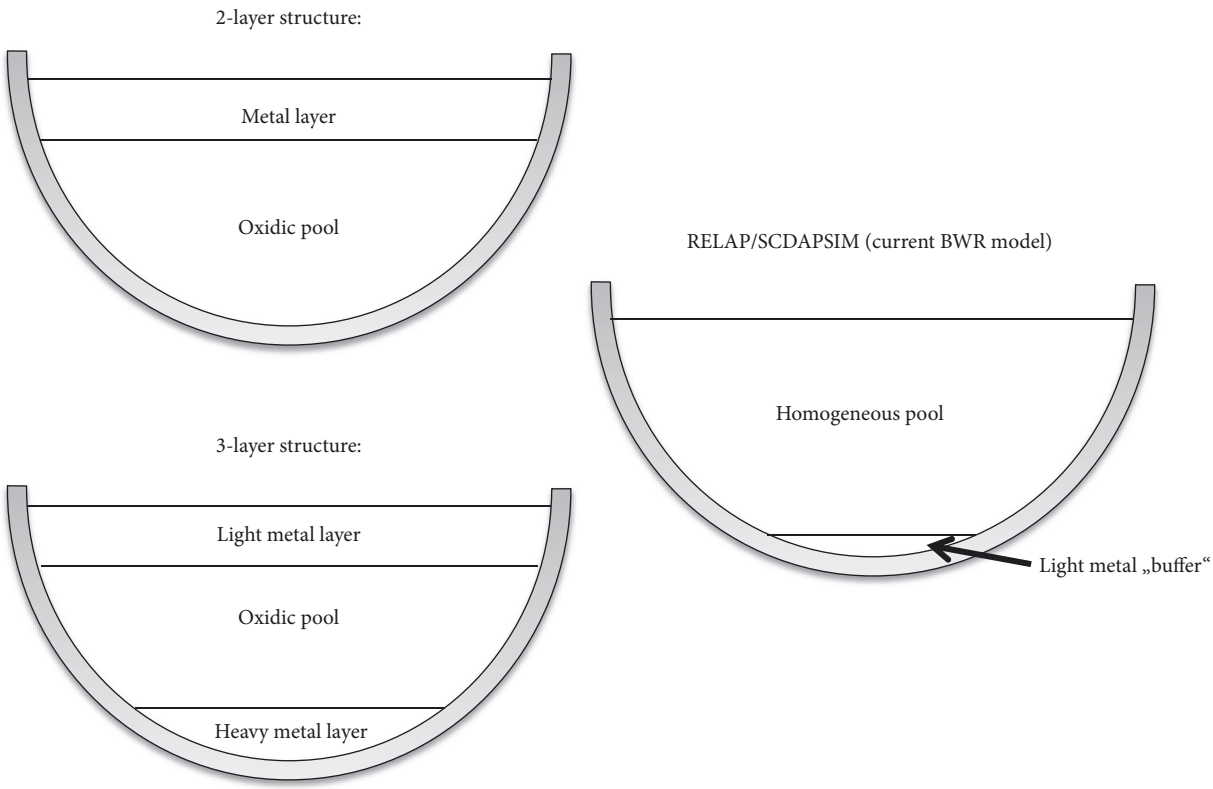

Figure 9: Layer formation in debris bed compared to RELAP/SCDAPSIM model.

coefficient", which is based on the Rayleigh number. The liquefied debris mass calculated by RELAP/SCDAPSIM in comparison with the total debris mass is presented in Figure 11. It can be seen from the figure that the debris bed contains approximately 80000 kg of molten material at around 7000 s after the beginning of the accident. Unfortunately, only one molten pool is considered in current RELAP/SCDAPSIM MOD 3.4 code version; therefore it cannot model the liquid light metal above the liquid oxidic pool which is a typical situation to have the "focusing effect" [22]. The influence of "focusing effect" is evaluated analytically in Section 4.4.

The temperature of the external RPV wall for all cases is shown in Figure 12. Internal wall temperature is shown in Figure 13. The heat flux from RPV to the water in reactor

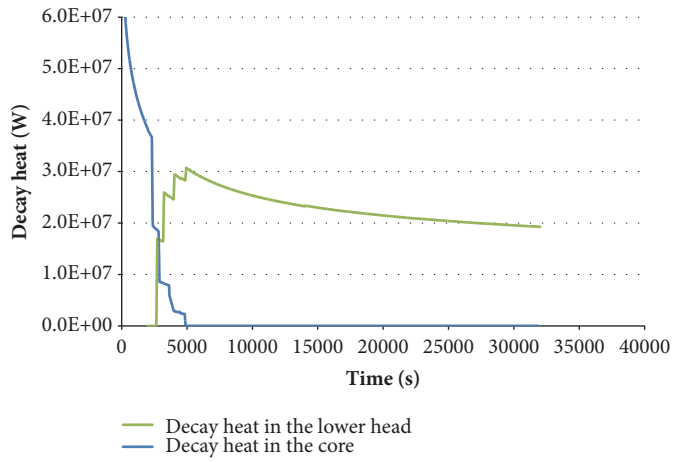

Figure 10: Decay heat in the reactor core and the corium in the lower head.

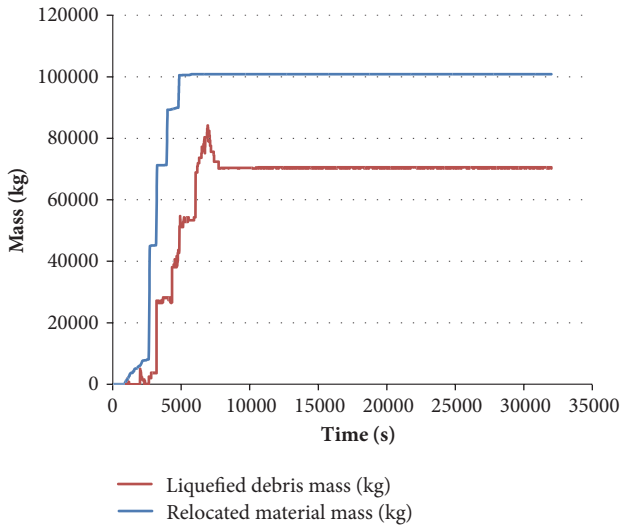

Figure 11: Liquefied debris mass in comparison with the total relocated material mass.

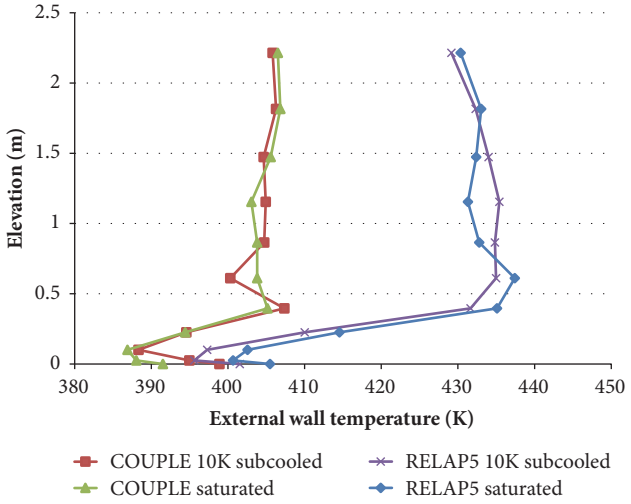

Figure 12: Maximum RPV external wall temperature for each case.

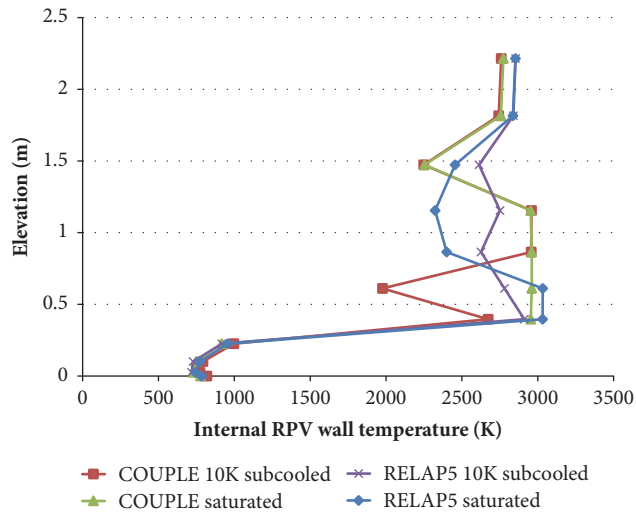

Figure 13: Maximum RPV internal wall temperature for each case.

cavity is shown in Figure 14. Also, the heat transfer coefficient is presented in Figure 15. The results are presented for the saturated or subcooled boiling using RELAP5 heat transfer mode (model shown in Figure 1(a)) and COUPLE heat transfer mode (model shown in Figure 1(b)).

Calculation results showed what the external surface successfully cooled and CHF is not expected with any of the heat transfer modes. As it is shown in Figure 14 there is a significant margin between CHF (which was calculated by (2)) and the calculated actual heat flux. The results suggest that main factor for the given reactor to achieve success with IVR strategy is to maintain the water level in the reactor pit.

As for the distribution of the heat fluxes/temperature/heat transfer coefficient along the wall, it can be observed that, in both heat transfer modes, heat flux at the bottom of the RPV is the lowest. This is due to the fact that there is no formation of the layers considered in RELAP/SCDAPSIM, and there is a light metal "buffer" (structure of thicker crust without the decay heat) at the bottom of the RPV, Figure 9.

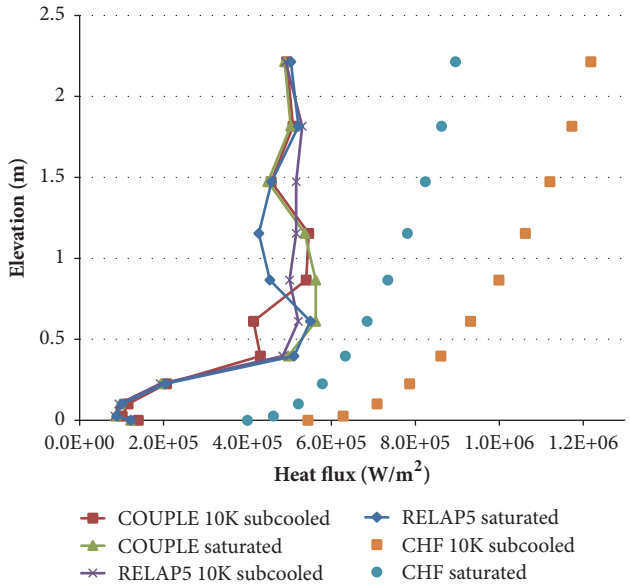

Figure 14: Maximum RPV heat flux to the ex-vessel for each case.

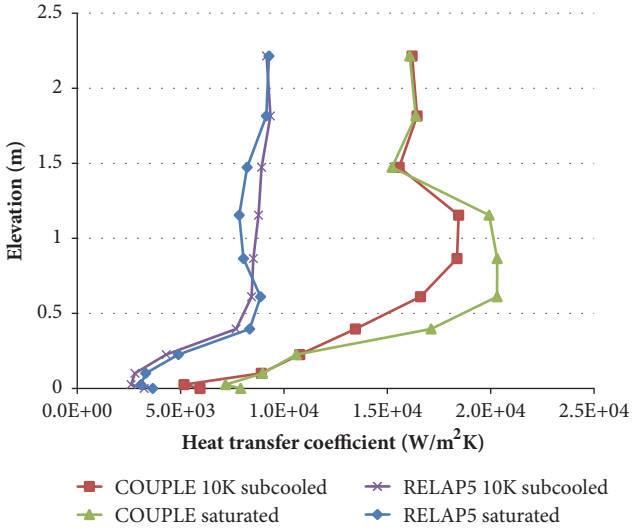

Figure 15: Heat transfer coefficient from external wall to ex-vessel volume for each case.

Going upwards along the RPV wall the results show that the COUPLE heat transfer mode is more effective and the heat transfer coefficient is higher (Figure 15). Therefore, the wall temperature (Figure 12) is also lower by around 30 K. The correlations for ex-vessel heat transfer implemented into COUPLE code are based on the experimental results for the shape of RPV lower head, submerged into a pool of water [10]. For this reason, employing the COUPLE based heat transfer mode is strongly recommended for such kind of problems, while RELAP5 calculated heat transfer effectiveness is considered underestimated. The underestimation can be seen in both saturated and 10 K subcooled cases. On the other hand, COUPLE heat transfer mode can be not suitable in some cases, since the HTC in a natural convection is not

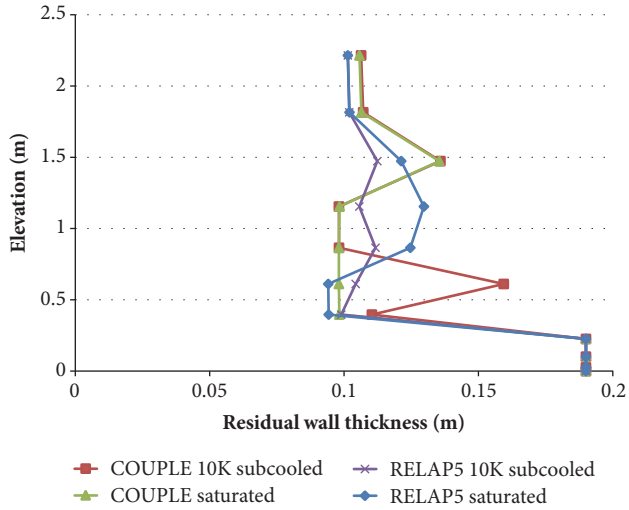

Figure 16: Residual wall thickness of the RPV for each case.

only strongly influenced by the shape of the lower head, but also the geometry of the cooling channel (the width, with/without baffle, and RPV coating). These aspects should be considered when applying COUPLE based heat transfer mode.

As it was mentioned at the beginning of Section 4, the main parameter for the RPV integrity would be the residual wall thickness. The results of the analysis are presented in Figure 16. The calculations were performed taking into account external wall temperature (Figure 12) and internal wall temperature (Figure 13) and assuming linear temperature gradient in the wall. As it can be seen from the results, the minimal residual wall thickness is calculated to be around 10 cm, which is sufficient to maintain the integrity of the RPV.

Summarizing the results it may be concluded that currently the RELAP/SCDAPSIM computer code can evaluate the effectiveness of IVR strategy only in case of the homogenous debris bed (as it is presented in Figure 9). The correlations for heat transfer from the external RPV surface are implemented into the code and are based on real experimental data. However, the models of the RELAP/SCDAPSIM computer code should be updated to evaluate more complex processes in the debris bed and the ability to predict typical 2 or 3 layers stratification of oxides and metals could give more realistic results. Predicting the focusing effect would enable evaluating local critical heat fluxes, which are potentially dangerous when using IVR strategy for severe accident management.

4.4. Analytical Solution for Metal Layers and Focusing Effect. As it was already mentioned, due to RELAP/SCDAPSIM limitations, this code does not take into account the debris separation into oxidic and metallic layers (shown in Figure 9). In order to bypass this limitation, the analytical study was carried out, assuming steady-state conditions in the lower head. This analytical study is based on the work done by

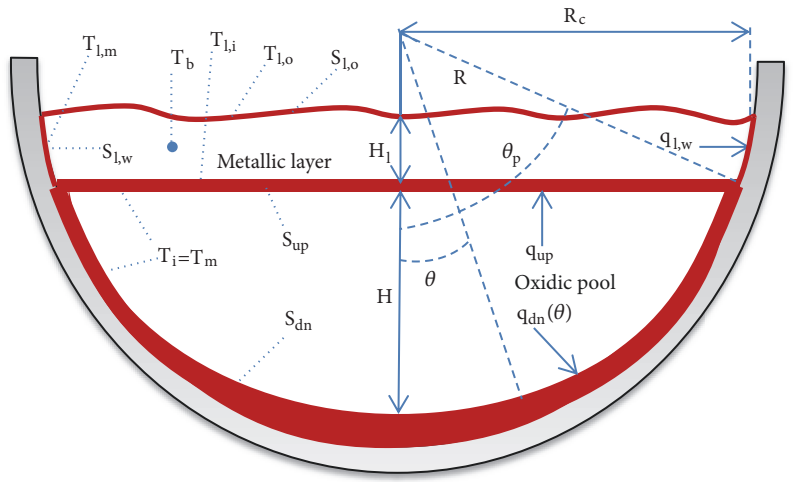

Figure 17: Graphical representation of parameters, used for solving the heat fluxes.

Theofanous et al. [2]. The sketch of the problem and variables is shown in Figure 17.

The heat transfer in the oxidic layer was calculated using the following:

$$Nu_{up} = 0.345 \cdot Ra'^{0.233}, \tag{3}$$

$$Nu_{dn} = 0.0038 \cdot Ra'^{0.35} \tag{4}$$

where Nu_{up} is the Nusselt number defining heat transfer to the metallic layer on the top of the oxidic layer and Nu_{dn} is the Nusselt number defining heat transfer to the vessel wall in contact with the oxidic layer. The power split between "up" and "down" regions is based on the assumption that the crust exists all around the oxidic pool and the interface temperatures of the upper boundary and side boundary are the same.

Ra' is the Rayleigh number with volumetric heating:

$$Ra' = Gr \cdot Pr \cdot Da \tag{5}$$

The dimensionless Grashof (Gr), Prandtl (Pr), and Damm-köhler (Da) numbers used in this equation are expressed as follows:

$$Gr = \frac{g\beta\left(T_{max} - T_i\right)H^3}{\nu^2};$$

$$Pr = \frac{\nu}{\alpha}; \tag{6}$$

$$Da = \frac{\dot{Q}H^2}{k\left(T_{max} - T_i\right)}$$

where g is acceleration due to gravity (m/s^2); β is thermal expansion coefficient (1/K); k is thermal conductivity (W/(m·K)); α is thermal diffusivity (m^2/s); ν is kinematic viscosity (m^2/s); T_{max} is bulk temperature of the fluid (K); T_i is temperature at the boundary (K); H is characteristic length or in our case layer height (m); $\dot{Q}$ is volumetric heat generation rate (W/m^3).

The heat transfer along the curved surface of the lower head depends on the contact angle, and to identify this heat transfer the correlations were used:

$$\frac{Nu_{dn}(\theta)}{Nu_{dn}} = 0.1 + 1.08\left(\frac{\theta}{\theta_p}\right) - 4.5\left(\frac{\theta}{\theta_p}\right)^2 + 8.6\left(\frac{\theta}{\theta_p}\right)^3, \quad 0.1 \le \frac{\theta}{\theta_p} \le 0.6, \tag{7}$$

$$\frac{Nu_{dn}(\theta)}{Nu_{dn}} = 0.41 + 0.35\left(\frac{\theta}{\theta_p}\right) + \left(\frac{\theta}{\theta_p}\right)^2, \quad 0.6 < \frac{\theta}{\theta_p} \le 1 \tag{8}$$

where θ is contact angle at location of interest (degrees); θ_p is contact angle at the top of the oxidic layer (degrees).

The distribution between heat fluxes to the sidewalls (q_{dn}) and to the metallic layer (q_{up}) is found by the following:

$$\dot{Q}V = S_{up} \cdot q_{up} + S_{dn} \cdot q_{dn} \tag{9}$$

where $\dot{Q}$ is volumetric heat generation rate of the oxidic layer (W/m^3); V is volume of the oxidic layer (m^3); S_{up} is contact area of the oxidic layer and the metallic layer.

After the oxidic layer is solved and the heat flux to the metallic layer (q_{up}) is found, the next step is to solve the heat fluxes in the metallic layer. The heat transfer in the metallic layer was calculated using Globe & Dropkin equation [23]:

$$Nu = 0.069 \cdot Ra^{1/3} \cdot Pr^{0.074} \tag{10}$$

Table 3: Inventories and basic properties of relocated materials.

Material	Mass (kg)	Density (kg/m^3)	Specific heat c_p (J/kg·K)	Volume (m^3)
UO2	79337	8740	485	9.08
ZrO2	5972	5990	815	1.00
Zr	12002	6130	458	1.96
Fe	3312	7020	835	0.47
		Volume averaged:	Mass averaged:	
Oxidic phase (UO2+ZrO2):	85309	8467.85	508.10	10.07
Metallic phase (Fe+Zr):	15314	6302.82	539.53	2.43
TOTAL:	100623			12.50

Table 4: Properties of oxidic and metallic layers assumed in analytical calculations.

Property	Notation (unit)	OXIDIC layer	METALLIC layer
Thermal expansion coefficient	β (1/K)	1.05E-04	1.10E-04
Thermal conductivity	k (W/m·K)	5.3	31.4
Dynamic viscosity	μ (Pa·s)	5.35E-03	4.00E-03
Emissivity (crust for Oxide and molten for Metallic)	ϵ	0.8	0.45
Liquidus temperature	T_i *or* $T_{l,m}$ (K)	2973	1600

From energy balance considerations, as shown by Theofanous et al. (with the Prandtl number ~0.13), we have the following:

$$(T_{l,i} - T_b)^{4/3} = (T_b - T_{l,o})^{4/3} + \frac{H_l}{R_c}(T_b - T_{l,m})^{4/3} \quad (11)$$

$$0.15 \cdot k \left(\frac{g \cdot \beta}{\alpha \cdot \nu}\right)^{1/3} (T_b - T_{l,o})^{4/3} = \epsilon \sigma T_{l,o}^4 \quad (12)$$

$$q_{up} = 0.15 \cdot k \left(\frac{g \cdot \beta}{\alpha \cdot \nu}\right)^{1/3} (T_{l,i} - T_b)^{4/3} \quad (13)$$

This system of three equations is solved to find three unknowns: T_b, $T_{l,i}$, and $T_{l,o}$. The lower indices here are referred to as follows: b, bulk; l,o, top surface of the metallic layer; l,m, liquidus; l,w – metallic layer interface with RPV wall. Other variables are as follows: ϵ, emissivity; σ, Stefan-Boltzmann constant (W·m^{-2}·K^{-4}); H_l, height of metallic layer (m); R_c, radius at the top location of metallic layer (m).

After solving the temperatures, the heat flux to the RPV wall ($q_{l,w}$) is found by the following:

$$q_{l,w} = 0.15 \cdot k \left(\frac{g \cdot \beta}{\alpha \cdot \nu}\right)^{1/3} (T_b - T_{l,m})^{4/3} \quad (14)$$

The initial data for inventories of relocated materials were taken from the results of RELAP/SCDAPSIM calculations. The properties of materials were assumed the same as in Theofanous et al. [2]. For this analysis only base values were used. The initial data of relocated materials is shown in Table 3. The resulting debris bed is shown in Figure 18. The height of metallic layer is only 0.15 m. The values of other properties for the oxidic and metallic layers are given in Table 4.

The comparison of local heat flux from RPV wall to water with the CHF values allows justifying if IVR strategy could be successfully applied. This heat flux is directly related to the decay heat in the lower head. As it can be seen from Figure 10, the maximum decay heat (~30 MW) is observed at around 5000 s after the accident. This decay heat is very conservative, because additional time is needed for stratification and melting of the internal structures in the lower head. Moreover, the loss of volatiles in the lower head is not taken into account. However, the decay heat of 30 MW was assumed as an extreme case. Moreover, there were no additional steel added, which should come from core plate,

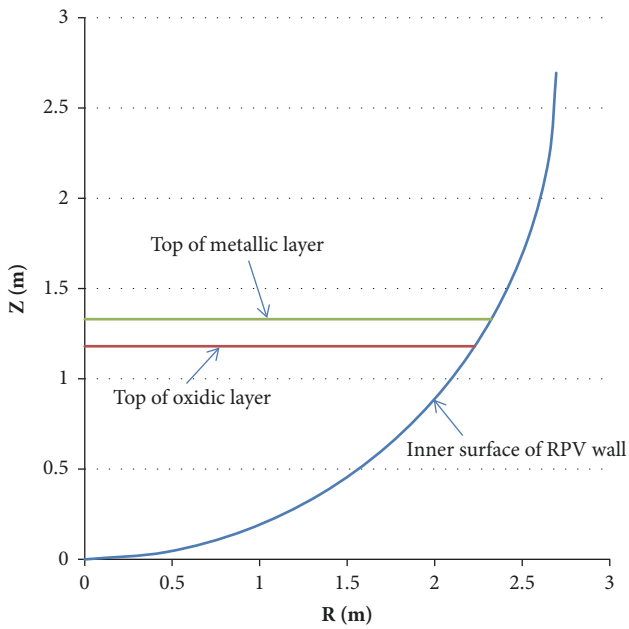

Figure 18: Graphical representation of oxidic and metallic layers in the RPV.

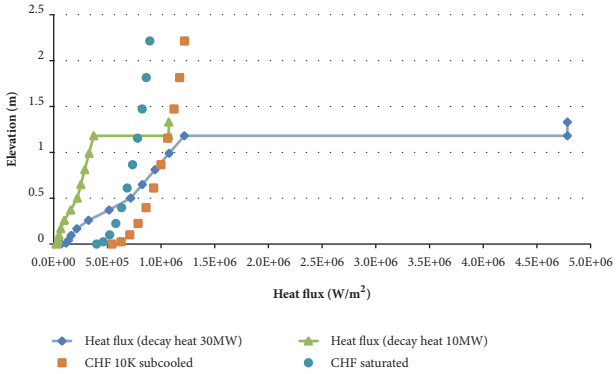

FIGURE 19: Calculated heat fluxes along the RPV wall. Decay heat 30 MW and 10 MW.

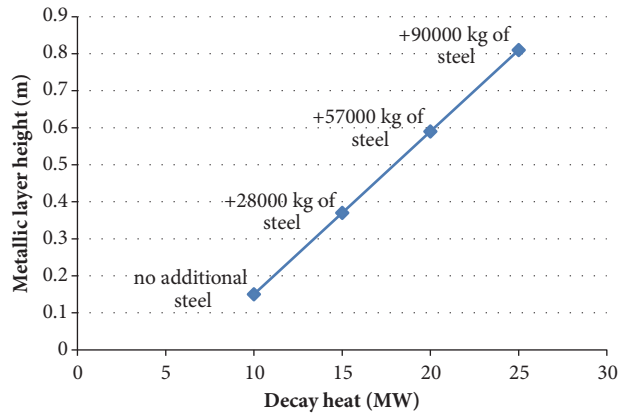

FIGURE 20: Decay heat versus metallic layer height, required to achieve heat flux equal to CHF.

internal structures in the lower head, and the ablated vessel wall. The analytical calculation results for this extreme case, i.e., heat flux along the RPV wall together with CHF curves, are shown in Figure 19. As it is presented in the figure, with the metallic layer being only 0.15 m, 30 MW decay heat is too high, and RPV failure is inevitable due to excessive heat flux of 4.8 MW/m^2. At the same time, it can be observed that, even within the oxidic layer, the heat flux exceeds the CHF. Therefore it could be concluded that IVR is not possible with 30 MW decay heat in such geometry of the lower head and such configuration of debris. It is shown in the same figure that in order to stay within the limits of subcooled boiling CHF (obtained by SBLB tests [20]), the decay heat should be less than 10 MW.

As it was demonstrated, the focusing effect is relatively high, but this is due to a very thin metallic layer, which is only 0.15 m. This case is not realistic, since more steel should be added from core plate and structures in the lower head. The total mass of stainless steel in control rod guide tubes and instrumentation guide tubes makes around 50,000 kg. Also, the ablated vessel wall would also eventually transfer to the metallic layer. Moreover, separation into oxidic and metallic layers takes time, and, during this time window, decay heat of molten materials also decreases. These transient processes are complicated and require detailed modelling, and in our case we must make more assumptions. For this reason, a parametric study has been conducted. In this parametric study, the oxidic layer was assumed the same in all cases; the target was to match the metallic layer heat flux and CHF of 10 K subcooled boiling. The CHF at the top of oxidic layer (height of 1.15 m) is equal to 1.06 MW/m^2, so the criterion was set that the heat flux from metallic layer cannot exceed this value. Following these conditions for each decay heat value (25 MW - 10 MW), the minimum metallic layer height was found. The results are shown in Figure 20. The additional mass of steel required to reach metal layer height in each case is also presented in Figure 20.

Figure 10 suggests that the decay heat after debris stratification could reach 20–25 MW. In order to maintain the heat flux below CHF, additional 57000–90000 kg of steel would be needed. The availability of molten steel and timing of debris stratification during transient should be analyzed with more capable software. The other aspect to consider in this approach is the CHF value itself, since higher values (up to ~1.8 MW/m^2) can usually be reached using improved design (with baffle, vessel coating, etc.). With more details on the reactor design (masses of the melted different metallic structures in the vessel and possibility of enhancing the efficiency of the ERVC), the results of this study should be updated.

5. Conclusions

The initiating event selected for the analysis was large break LOCA with total failure of cooling water injection in a BWR-5 reactor in Mark-II containment with initial nominal power of ~2000 MWt. In this most conservative scenario, no activation of emergency water supply system was assumed. This hypothetical scenario leads to the very fast overheating of the core and the start of fuel melting at high decay heat level (~600 seconds after the beginning of the accident). The dry-out of the lower head occurs approximately 1 hour after beginning of the accident. It was assumed in the simulation that the reactor cavity (pit) around the reactor vessel is flooded by water in advance. To evaluate RELAP/SCDAPSIM ability to model ex-vessel heat transfer, two modes were analyzed, i.e., (a) RELAP5 based heat transfer mode and (b) COUPLE based heat transfer mode.

It was observed that using RELAP5 based heat transfer mode the RPV wall temperature was overestimated, compared to the COUPLE based heat transfer mode. The correlations for ex-vessel heat transfer implemented into COUPLE computer code are based on the experimental results for the shape of RPV lower head, submerged into a pool of water. For this reason, employing the COUPLE based heat transfer mode is strongly recommended for such kind of problems. However, it must be noted that COUPLE heat transfer mode can be not suitable in some cases, e.g., specific geometry of the cooling channel and RPV coating.

RELAP/SCDAPSIM does not take into account the formation of the metallic layer on the top of the oxidic layer. For this reason, some important effects (such as focusing effect)

are not considered and the local heat fluxes are underestimated using this tool. Using the homogenous pool models, the results show that even for the most conservative initial and boundary conditions critical heat flux is not reached in the analyzed cases. To investigate the influence of debris separation into oxidic and metallic layers on the heat transfer through RPV wall and to evaluate the substantiation of received optimistic RELAP/SCDAPSIM calculation results, the analytical study was conducted. The analytical study presented in this paper showed that, considering oxidic and metallic layers, a relatively thin metallic layer (0.15 m), and maximum decay heat (30 MW), the steady-state heat flux in the metallic layer greatly exceeds the CHF value. The metallic layer height is calculated from the results of RELAP/SCDAPSIM, taking into account only steel in the reactor core, and 30 MW is the peak power calculated by RELAP/SCDAPSIM at the time of slumping. Since these values are not realistic during actual accident scenario, a parametric study has been conducted to identify metallic layer height needed to dissipate heat at lower rate than CHF. The results show that a significant amount of steel should be added (57000–90000 kg) in order to stay below CHF (1.06 MW/m^2) in case of decay heat of 20–25 MW. This amount of steel could be acceded from core plate and structures in the lower head and ablated vessel wall. Unfortunately at this moment there is no possibility of precisely evaluating the amount of the steel which could be relocated to the lower head during the postulated accident.

The models of the RELAP/SCDAPSIM computer code are recommended to be updated to evaluate more complex processes in the debris bed and the ability to predict typical 2 or 3 layers stratification of oxides and metals could provide more realistic results.

The work presented in this article is a part of the IVMR project, which was launched with the objective to investigate the applicability of IVR as a strategy for severe accident management in nuclear reactors. The whole spectrum of different reactors will be investigated and the developed computational tools for predicting and defining their reliability will be a significant result of this project. The results of this project will be used as a strong background in the safety analysis, when implementing this strategy in real nuclear power plants, especially with high power reactors.

Data Availability

The data used to support the findings of this study are included within the article.

Conflicts of Interest

The authors declare that they have no conflicts of interest.

Acknowledgments

The work is performed in the frame of Project "In-Vessel Melt Retention Severe Accident Management Strategy for Existing and Future NPPs", IVMR, under H2020 Grant Agreement no. 662157. The authors would like to thank Dr. Javier Ortiz-Villafuerte (Nuclear Systems, National Institute of Nuclear Research, Mexico) for his considerable advice and providing information regarding mass of steel in control rod and instrumentation guide tubes.

References

[1] H. Tuomisto and T. G. Theofanous, "A consistent approach to severe accident management," *Nuclear Engineering and Design*, vol. 148, no. 2-3, pp. 171–183, 1994.

[2] T. G. Theofanous, C. Liu, S. Additon, S. Angelini, O. Kymäläinen, and T. Salmassi, "In-vessel coolability and retention of a core melt," *Nuclear Engineering and Design*, vol. 169, no. 1-3, pp. 1–48, 1997.

[3] O. Kymäläinen, H. Tuomisto, and T. G. Theofanous, "In-vessel retention of corium at the Loviisa plant," *Nuclear Engineering and Design*, vol. 169, no. 1-3, pp. 109–130, 1997.

[4] H. Esmaili and M. Khatib-Rhabar, *NUREG/CR-6849, Analysis of In-Vessel Retention and Ex-Vessel Fuel Coolant Interaction for AP1000*, 2004.

[5] J. L. Rempe, D. L. Knudson, K. G. Condie, K. Y. Suh, F.-B. Cheung, and S.-B. Kim, "Corium retention for high power reactors by an in-vessel core," *Nuclear Engineering and Design*, vol. 230, no. 1-3, pp. 293–309, 2004.

[6] D. L. Knudson, J. L. Rempe, K. G. Condie, K. Y. Suh, F.-B. Cheung, and S.-B. Kim, "Late-phase melt conditions affecting the potential for in-vessel retention in high power reactors," *Nuclear Engineering and Design*, vol. 230, no. 1-3, pp. 133–150, 2004.

[7] H. Schmidt, W. Brettschuh, J. Meseth et al., "Tests to investigate the RPV exterior two-phase flow behavior in the event of core melt," in *Proceedings of the 38th European Two-Phase Flow Group Meeting*, Paper A6, Karlsruhe, Germany, 2000.

[8] L. A. Dombrovskii, V. N. Mineev, A. S. Vlasov et al., "In-vessel corium catcher of a nuclear reactor," *Nuclear Engineering and Design*, vol. 237, no. 15-17, pp. 1745–1751, 2007.

[9] F. Fichot, L. Carénini, M. Sangiorgi et al., "Some considerations to improve the methodology to assess In-Vessel Retention strategy for high-power reactors," *Annals of Nuclear Energy*, vol. 119, pp. 36–45, 2018.

[10] L. Siefken, E. Coryell, S. Paik, and H. Kuo, "SCDAP/RELAP5 Modeling of Heat Transfer and Flow Losses in Lower Head Porous Debris," INEEL/EXT-98-00820, Rev. 2, 1999.

[11] G. Espinosa-Paredes and A. Nuñez-Carrera, "SBWR model for steady-state and transient analysis," *Science and Technology of Nuclear Installations*, vol. 2008, Article ID 428168, 18 pages, 2008.

[12] C. Allison, J. Hohorst, F. Venturi, N. Forgione, and R. Lopez, "Application of RELAP/SCDAPSIM/MOD3.5 to a Representative BWR for Fukushima-Daichii-like SBO transients," in *Proceedings of the International Congress on Advances in Nuclear Power Plants, ICAPP 2013*, 2013.

[13] G. Espinosa-Paredes, R. Camargo-Camargo, and A. Nuñez-Carrera, "Severe accident simulation of the laguna verde nuclear power plant," *Science and Technology of Nuclear Installations*, vol. 2012, Article ID 209420, 11 pages, 2012.

[14] M. M. Gris, "Reactor Pressure Vessel Neutron Embrittlement & Metal fatigue," in *Materials Degradation Technical Meeting*, Vienna, Austria, 2013.

[15] Bock. Module 06 Boiling Water Reactors (BWR), 2016.

[16] M. J. Fallacara, *Hardened Containment Vents for BWR Mark I & II Containments and Evaluation of Filtration Systems*, Rensselaer Polytechnic Institute Hartford, Connecticut, USA, 2013.

[17] C. M. Allison, G. A. Berna, E. W. Coryell et al., "SCDAP/RELAP5 Users Guide and Input Manual," NUREG/CR-6150 EGG-2720, Idaho National Engineering Laboratory, USA, 1998.

[18] C. M. Allison, G. A. Bema, T. C. Cheng et al., "SCDAP/RELAP5/MOD 3.2 code manual volume II: damage progression model theory," NUREG/CR-6150 INEL-96/0422, Idaho National Engineering and Enviromental Laboratory, New York, NY, USA, 1997.

[19] A. Nuñez-Carrera, R. Camargo-Camargo, G. Espinosa-Paredes, and A. López-García, "Simulation of the lower head boiling water reactor vessel in a severe accident," *Science and Technology of Nuclear Installations*, vol. 2012, Article ID 305405, 8 pages, 2012.

[20] F. Cheung, K. Haddad, and Y. Liu, "Critical heat flux (CHF) phenomenon on a downward facing curved surface," NUREG/CR6507, 1997.

[21] R. Park, K. Kang, S. Hong, S. Kim, and J. Song, "Corium behavior in the lower plenum of the reactor vessel under IVR-ERVC condition: Technical issues," *Nuclear Engineering and Technology*, vol. 44, no. 5, pp. 237–248, 2012.

[22] X. Wang and X. Cheng, "Analysis of Focusing Effect of Light Metallic Layer in Stratified Molten Pool Under IVR-ERVC Condition," *Journal of Nuclear Engineering and Radiation Science*, vol. 1, no. 2, article 021007, 2015.

[23] S. Globe and D. Dropkin, "Natural-convection heat transfer in liquids confined by two horizontal plates and heated from below," *Journal of Heat Transfer*, vol. 81, no. 24, 1959.